Characterization of *P. falciparum* dipeptidyl aminopeptidase 3 specificity identifies different amino acid preferences between peptide-based substrates and inhibitors.

Edgar Deu[1,*], Laura E. de Vries[1], Mateo Isidrio Sanchez[2], Katarzyna Groborz[3], Laurie Kuppens[1], Marcin Poreba[3], Christine Lehmann[1], Fang Yuan[4], Shirin Arastu-Kapur[4], Matthew Bogyo[4], Marcin Drag[3].

[1]Chemical Biology Approaches to Malaria Laboratory, The Francis Crick Institute, London, England, Unite Kingdom.

[2]Department of Chemistry, Universidad de Santiago de Compostela, Santiago de Compostela, Spain.

[3]Division of Bioorganic Chemistry, Faculty of Chemistry, Wroclaw University of Technology, Wroclaw, Poland.

[4]Department of Pathology, Stanford University School of Medicine, Stanford, United States.

*Corresponding author:

e-mail: edgar.deu@crick.ac.uk

Tel: +44 (0) 20 3796 1412

ABSTRACT

Dipeptidyl aminopeptidases (DPAPs) are druggable cysteine proteases that cleave dipeptides from the N-terminus of proteins and oligopeptides. *Plasmodium* DPAPs have been shown to be important for the asexual replication of the malaria parasite and are therefore potential antimalarial targets. DPAP1 seems to be important for parasite growth within infected red blood cells, and DPAP3 plays a critical role in the invasion of erythrocytes by the malaria parasite. An inhibitor able to block both of these proteases will target the parasite at different developmental stages thus making the emergence of drug resistance more difficult. Understanding the substrate specificity of these proteases is important to understand their molecular function and to help develop potent and selective inhibitors. In this study, we used peptide-based libraries of substrates to determine the specificity of DPAP3 and compared it to that of DPAP1 and human cathepsin C (mammalian DPAP homologue). We then used the structure activity relationships information from these screens to develop optimal DPAP3 fluorogenic substrates as well as highly specific DPAP1 and DPAP3 inhibitors. Interestingly, while the substrate specificity of a protease is often used to develop potent inhibitors, in this study we show that equally potent and highly specific inhibitors can be developed based on the structure of poor substrates. Overall, this study illustrates that focusing the development of peptidic inhibitors solely on the substrate specificity of a protease might overlook important structural features that can be exploited to developed highly potent and selective compounds.

Malaria is a devastating infectious parasitic disease causing close to half a million deaths every year[1]. Over the last 15 years the world has seen a very significant drop in malaria incidence, mainly due to the global distribution of insecticide-impregnated bed nets and the use of artemisinin-based combination therapies as the standard of care for uncomplicated malaria[2]. However, malaria remains a major global health burden with half of the world population at risk and around 200 million clinical cases per year. Unfortunately, mosquitoes are becoming resistance to insecticides[3] and artemisinin resistance is on the rise[4], thus making the identification of antimalarial targets and the development of drugs with novel mechanisms of action extremely urgent[5].

Malaria is caused by parasites of the *Plasmodium* genus and is transmitted by Anopheles mosquitoes during a blood meal. Upon infection, malaria parasites first establish an asymptomatic infection in the liver before reaching the blood stream where they replicate asexually through multiple rounds of red blood cell (RBC) invasion, intracellular growth and division, and egress from infected RBCs (iRBCs). A small proportion of parasites will develop into male and female gametocytes that will sexually reproduce in the mosquito midgut after being swallowed during a blood meal. After transversal of the midgut epithelial, parasites replicate and travel to the salivary gland from where they will be transmitted to another human host. The exponential asexual replication of the parasite in the blood stream is responsible for all the clinical manifestations and pathology of this disease.

Dipeptidyl aminopeptidases (DPAPs) are papain-fold cysteine proteases that are expressed at all stages of parasite development[6,7] and might therefore be viable drug targets to treat malaria and prevent its transmission, especially if pan-DPAP inhibitors can be developed. DPAPs recognize the free N-terminus of protein substrates and cleave N-terminal dipeptides[8,9]. The mammalian homologue cathepsin C (CatC) is the best studied DPAP and in most cells it plays a catabolic lysosomal function. However, in some immune cells it is responsible for activating a family of secretory serine proteases involved in the immune response and inflammation such as neutrophil elastase, granzyme A and B, or cathepsin G[10-13]. Because of its role in activating pro-inflammatory proteases, CatC has been pursued by the pharmaceutical industry as a potential target for chronic inflammatory diseases[14-16]. Indeed, phase I clinical trials with CatC inhibitors have been performed by GSK (GSK2793660)[17] and

Astrazeneca (AZD-7986; https://clinicaltrials.gov/ct2/show/study/NCT02653872) for the treatment of bronchiectasis, thus proving that DPAPs can be targeted with small drug-like molecules.

Three DPAPs are conserved across *Plasmodium* species but very little is known about their molecular functions. In *P. falciparum*, the most virulent *Plasmodium* species, attempts to directly knockout (KO) DPAP1[18] or DPAP3[19] have been unsuccessful, suggesting that they are important for parasite replication. In the *Plasmodium berghei* murine model of malaria KO of DPAP1 or DPAP3 results in a significant decrease in parasite replication *in vivo*[20-22]. Finally, KO of *P. falciparum* DPAP2, which is only expressed in sexual stages, results in a very significant decrease in gametocyte egress from iRBCs, suggesting that DPAPs might be potential drug target to block malaria transmission[23]. Interestingly, a two-fold increase in DPAP1 expression was observed in DPAP2 KO parasites[24], suggesting that DPAP1 might be able to compensate for the loss of DPAP2.

DPAP1 localizes mainly in the digestive vacuole[18], an acidic organelle where degradation of haemoglobin takes place. This catabolic pathway provides a source of amino acids for protein synthesis and liberates space within the RBC for parasite growth. Phenotypic characterization of the effect of DPAP1 inhibitors is consistent with this function and overall suggests that DPAP1 activity is important for intracellular parasite growth[25]. Previously published inhibition studies on DPAP3 suggested that this protease was at the top of the proteolytic cascade that controls parasite egress form iRBCs[26]. However, our recent conditional KO studies have disproven this hypothesis and shown that DPAP3 is only critical for efficient RBC invasion[19]. We also showed that DPAP3 localizes in apical secretory organelles and that it is released immediately before parasite egress[19]. Overall, developing pan-DPAP inhibitors as antimalarial drugs will target the parasite at different stages of parasite development and might slow down the emergence of resistance due to its polypharmacological mode of action.

A good understanding of the specificities of *Plasmodium* DPAPs and CatC is required in order to develop pan-DPAP inhibitors with minimal off target effects on host CatC, and to design highly specific DPAP1 and DPAP3 inhibitors to study the biological function of these proteases. A general approach to determine the specificity of proteases upstream of the scissile bond

(non-prime pockets) is the use of positional scanning substrate libraries where a fluorophore is conjugated to the C-terminal of a collection of peptides *via* an amide bond. Proteolytic cleavage of this bond results in a very significant increase in fluorescence intensity and allows accurate measurement of substrate turnover in a continuous assay. The most common libraries used to determine the specificity of proteases are positional scanning synthetic combinatorial libraries (PS-SCL)[27-29]. PS-SCL are composed of multiple sub-libraries designed to determine the specificity at each non-prime binding pocket in a protease. In each sub-library, the amino acid at a specific position is varied while a stoichiometric mixture of all natural amino acids is used in all other positions. PS-SCL thus provide the substrate specificity at each non-prime site in the context of all possible combination of amino acids at all the other sites. Alternatively, the specificity at a specific binding pocket can be determined by varying the identity of the amino acid at that position while fixing the rest of the peptide to residues known to be recognized by the protease of interest. This approach has been used to fingerprint the specificity of amino exopeptidases such as aminopeptidases[30,31] or DPAPs[32], which only recognise one or two amino acids upstream of the scissile bond, respectively. Similar positional scanning strategies have been applied to protease inhibitor libraries where the fluorophore is replaced with a reversible or irreversible warhead[33]. Optimum substrates and inhibitors are then designed by combining the best residues in each position. Importantly, the recent incorporation of non-natural amino acids into these libraries has very significantly increased the chemical space that can be explored to characterize the specificity of proteases and has allowed the design of more specific substrates and inhibitors[34-36].

Structure-activity relationship (SAR) studies with positional scanning substrate and inhibitor libraries have been performed both on DPAP1 and CatC[25,37,38], but to a much lesser extent on DPAP3[26]. Here, we use recombinant DPAP3 (rDPAP3) to screen libraries of peptide-based substrates and inhibitors and determine the specificity of DPAP3 at the P1 and P2 positions. These libraries are composed of a variety of natural and non-natural amino acids at one position while fixing the other position to a single amino acid known to be recognized by this family of proteases. Importantly, the libraries used in this study have been previously screened against DPAP1 and CatC and are therefore ideal to compare the specificities of these three proteases[32]. Our studies show that DPAP3 preferentially cleaves after basic and large aromatic residues (P1 position) and that it prefers substrates having N-terminal aliphatic

residues (P2 position). We also identified several non-natural N-terminal amino acids that are exclusively recognized by either DPAP1 or DPAP3. Interestingly, while structure-activity relationship (SAR) information obtained from positional scanning substrate libraries is often used to develop potent protease inhibitors[36], here we show that there are significant differences in specificity between substrates and inhibitors. Substrates containing N-terminal aromatic residues are cleaved very poorly by DPAP3 but are ideal to develop highly potent and selective inhibitors. Finally, by combining the SAR information obtained from the substrate and inhibitor screens we developed better DPAP3 substrates and highly selective DPAP1 and DPAP3 inhibitors that are able to inhibit their targets in live parasites. Overall, our study illustrates how positional scanning substrate libraries might not always identify optimal amino acids for inhibitor development.

MATERIALS AND METHODS

Reagents

The synthesis of the DPAP substrate library and that of the Val-Arg-ACC, Phe-Arg-ACC, and Tyr(NO_2)-hPhe-ACC[37 38] have been previously described. Additional substrates used in this study are described in the supplementary materials and were synthesized following previously published methods[32,39]. The synthesis of the DPAP inhibitor library, SAK2, SAK1, *L*-WSAK and *D*-WSAK were also previously described[26 19] were also previously described. The additional DPAP inhibitors used in this study were synthesized following a similar method[40]. The synthesis and characterization of these inhibitors and its synthetic intermediates is described in detail in the supplementary methods. The Phe-Arg-βNA and Gly-Arg-AMC substrates was purchase from Sigma.

Recombinant DPAP3 active site titration.

Recombinant DPAP3 was expressed in SF9 insect cells and purified from the culture supernatant by sequential ion exchange, Ni-NTA, and size exclusion chromatography as previously described[19]. To accurately determine the concentration of active rDPAP3 in our enzyme stocks we used activity-based probes (ABPs). ABPs are small molecule reporters of activity that use the catalytic mechanism of the targeted enzyme to covalently modify its active site. A reporter tag, usually a fluorophore or a biotin, allows for visualization and

quantification of the labelled enzyme in a gel-based assay[41]. Because ABPs only react with the active form of an enzyme and covalently modify its active site, in this case the catalytic Cys, they can be used to perform accurate active site titrations.

Our stock of rDPAP3 was diluted 20-fold in assay buffer (100 mM sodium acetate, 100 mM NaCl, 5 mM $MgCl_2$, 1 mM EDTA, 0.1% CHAPS, and 5 mM DTT at pH 6), pre-treated for 30 min with DMSO or 1 μM SAK1 (a DPAP3 covalent inhibitor), and rDPAP3 labelled with the DPAPs 1 μM FY01 for 1 h at RT. (FY01 is a cell-permeable fluorescent ABP that was initially developed for CatC[42] but that has also been shown to label *Plasmodium* DPAPs[25,26].) These samples were run on an SDS-PAGE gel along with a serial dilution of free probe (1.5-100 nM). In-gel fluorescence was measured using a Biorad PharosFX flat-bed scanner and the intensity of the fluorescent bands quantified using ImageJ. The fluorescent signal from the free probe was used as a calibration curved and compared to the difference in signal between the DMSO and SAK1 treated rDPAP3 (Fig. 1). Using this method, we determined that our stock concentration contained 840 nM of active rDPAP3.

Substrate turnover assay.

The substrate library was screened in triplicate at 1 μM substrate and 1 nM rDPAP3 in assay buffer. Substrate turnover was measured over 30 min at RT using a SpectroMax M5e plate reader (λ_{ex} = 355 nm, λ_{em} = 460 nm, emission filter 455 nm, for ACC (7-amino-4-carbamoylcoumarin) or AMC (7-amino-4methylcoumarin) substrates; λ_{ex} = 315 nm, λ_{em} = 355 nm, emission filter 420 nm, for Phe-Arg-βNA). Calibration curves of free βNA (β-napthylamide) and ACC (0-500 nM) under the same assay conditions were preformed to convert the turnover rate measured as fluorescent units per second into moles per second. The determine k_{cat} and K_m values, substrate turnover was measured at different substrate concentrations and initial velocities fitted to the Michaelis Menten equation (Eq. 1). The data was also fitted to Eq. 2 to obtain accurate k_{cat}/K_m values. A minimum of three replicates were performed for each substrate.

$$\frac{V_i}{Et} = \frac{k_{\mathrm{cat}} \cdot [\mathrm{S}]}{K_{\mathrm{m}} + [S]} \qquad \text{Eq. 1}$$

$$\frac{V_i}{Et} = \frac{(k_{\mathrm{cat}}/K_{\mathrm{m}})\cdot[\mathrm{S}]}{1+\frac{[S]}{K_{\mathrm{m}}}} \qquad \text{Eq. 2}$$

Irreversible inhibition assay.

To determine the inhibition constant of vinyl sulfone inhibitors against rDPAP3, 0.35 μM of nVal-nLeu(o-Bzl)-ACC (0.25 x K_m) was mixed with a dose response of inhibitor in assay buffer, and the turnover rate measure over 40 min at RT after addition of 0.2 nM rDPAP3. The data was fitted to the irreversible inhibition model shown in Eq. 1:

$$\mathrm{E} + \mathrm{I} \overset{K_{\mathrm{i}}}{\rightleftarrows} \mathrm{E{:}\,I} \overset{k_{\mathrm{inact}}}{\rightarrow} E - I \qquad \text{Eq. 3}$$

K_i is the inhibition equilibrium constant, and k_{inact} the rate of covalent modification of the catalytic Cys.

The progress curves (fluorescent units vs. time) were fitted to Eq. 4, where F is the measured fluorescence at time t, F_0 the initial fluorescence, V_0 the initial turnover rate, and k_{obs} the observed second order rate constant of inhibition measured at each inhibitor concentration[43].

$$(\mathrm{F} - \mathrm{F}_0) = V_0 \frac{1-e^{-k_{\mathrm{obs}}\cdot \mathrm{t}}}{k_{\mathrm{obs}}} \qquad \text{Eq. 4}$$

k_{obs} values where then fitted to Eqs. 5 or 6. to obtain the k_{inact} and K_i or k_{inact}/K_i values, respectively.

$$k_{\mathrm{obs}} = \frac{k_{\mathrm{inact}}\cdot[\mathrm{INH}]}{K_{\mathrm{i}}+[\mathrm{INH}]} \qquad \text{Eq. 5}$$

$$k_{\mathrm{obs}} = \frac{(k_{\mathrm{inact}}/K_{\mathrm{i}})\cdot[\mathrm{INH}]}{1+\frac{[\mathrm{INH}]}{K_{\mathrm{i}}}} \qquad \text{Eq. 6}$$

Inhibition constants for DPAP1 and CatC (R&D Systems) were determined in a similar way but using 0.25 x K_m concentration of the Pro-Arg-AMC (20 μM) and Gly-Arg-AMC (15 μM), respectively. Inhibition of DPAP1 was directly measured in parasite lysates using the DPAP1-selective substrate Pro-Arg-AMC[44].

Measurement of inhibitor specificity in biological samples.

Inhibition of *Plasmodium* DPAPs and the falcipains in intact parasites was measured using the FY01 ABP in competition assays as previously described[25,26]. The falcipains (FPs) are clan CA Cys proteases involved in haemoglobin degradation (FP2, FP2' an FP3)[45] and possibly RBC invasion (FP1)[46,47]. Briefly, 5 μL of percoll-purified schizonts were diluted in 45 μL of RPMI (Gibco), pre-treated for 30 min with a dose response of inhibitor, and labelled for 1 h with 1 μM FY01. Samples were then boiled for 10 min after addition of loading buffer and run on a 12% SDS-PAGE gel. Fluorescently labelled proteases in the gel were detected using a Biorad PharosFX flatbed fluorescence scanner. Because DPAP3 is only expressed late during the erythrocytic cycle[6], labelling in intact parasites was performed on very mature schizonts arrested 15-30 min before egress using 1 μM of the cGMP-dependent protein kinase inhibitor Compound 2[48]. These conditions ensured maximal level of DPAP3 activity and consistent FY01 labelling of DPAP3 in live parasites.

RESULTS

DPAP3 Substrate Specificity.

A positional scanning library of 96 substrates composed of a P1 sub-library of 39 substrates with a fixed P1 homophenylalanine (hPhe) residue and a P2 sub-library of 57 substrates with a fixed P2 Met residue (Fig. 2A) was screened against purified rDPAP3 at 1 μM, which is the same substrate concentration that was used to screen this library against DPAP1 and CatC[32]. The heat map shown in Fig. 1B compares the specificities of DPAP3 with those previously obtained for DPAP1 and CatC[32]. Note that the P2 library contained 18 substrates with a *D*-amino acid in P2: those corresponding to codon-coding amino acids except Gly, *D*-Cys, *D*-Met and *D*-Ile, plus *D*-hPhe and *D*-Phg (*D*-phenylglycine). Only the substrate containing the latter

residue was cleaved by rDPAP3. The data corresponding to the remaining 17 substrates having a *D*-amino acid in P2 was not included in Fig. 1.

All three DPAPs show broad and similar P1 specificity, which is not surprising because in clan CA proteases the P1 residue side chain is generally exposed to the solvent. For all DPAPs, a general preference for long basic, aliphatic, and aromatic P1 residues was observed—basic: Lys, Arg, homoarginine (hArg), or nitroarginine (Arg(NO_2)); aliphatic: Met, norvaline (nVal) and Leu; aromatic: hPhe, (4-benzothiazol-2-yl)homoalanine (hAla(Bht)), 6-benzyloxynorleucine (nLeu(o-Bzl)), glutamic acid benzyl ester (Glu(Bzl)), or homoserine-*O*-benzyl (hSer(Bzl))—. Interestingly, DPAP1 differs from CatC and DPAP3 in that it does not accept large hydrophobic groups such as cyclohexylalanine (Cha), 2-naphthalene (2Nal), biphenylalanine (Bip), 4-benzoyl-phenylalanine (Bpa), tyrosine-*O*-benzoyl (Tyr(Bzl)), or 4-guanidino-phenylalanine (Phe(guan)) in P1. Unfortunately, we could not identify any P1 residue that was recognized by *Plasmodium* DPAP1 and/or DPAP3 but not by CatC.

Clear differences in specificity were observed between the different DPAPs at the P2 position. Overall, DPAP3 seems to have a narrower P2 specificity among natural amino acids than DPAP1 or CatC, probably reflecting that DPAP3 has a more specific biological function in RBC invasion compared to the catabolic functions of DPAP1 and CatC. Both DPAP1 and DPAP3 have a strong preference for long aliphatic residues such as Leu, Ile, norleucine (nLeu), Met, or norvaline (nVal). Some non-natural amino acids seem to be exclusively cleaved by DPAP3 such as cyclohexylglycine (Chg), Phg, or 4-methyl-phenylalanine (Phe(Me)). Surprisingly, Phe(Me) is the only substrate in the library with an aromatic P2 residue that is turned over by DPAP3 even though vinyl sulfone inhibitors with a P2 aromatic residues such as Tyr, Trp, or nitrotyrosine (Tyr(NO_2)) have been shown to be potent DPAP3 inhibitors[19,26]. Interestingly, an Ile in P2 seems to by efficiently cleaved by both *Plasmodium* DPAPs but not by CatC.

Development of optimum DPAP3 substrates

To determine how P1 and P2 side chains influence the k_{cat} and K_m value of DPAP3 substrates, Michaelis Menten steady-state kinetics were performed on selected substrates from the P1 and P2 libraries. In addition, we synthesized a series of substrates by combining optimal natural and non-natural amino acids for DPAP3: Arg, hPhe, nLeu(o-Bzl), and Bpa in P1, and

Leu, Val, nVal, and Phg in P2. We also tested substrates predicted to be DPAP1-selective (Pro-Arg-ACC and hPro-hPhe-ACC) against rDPAP3. Finally, because we were surprised by the lack of DPAP3 activity observed for substrates with aromatic P2 residues, we tested Phe-Arg-AMC and Tyr(NO_2)-hPhe-ACC. The sequence of the latter is based on the structure of SAK1 (Tyr(NO_2)-hPhe-VS), which is the most potent DPAP3 inhibitor identified so far (see below). Table 1 and Fig. 1D report the Michaelis Menten parameters determined for all these substrates (Fits are shown in Fig. S1).

P1 residues have a significant influence in k_{cat}, with nLeu(o-Bzl) and long positively charged residues having the highest values. Interestingly, a positive charge on the δ position (Arg and Arg(NO_2)) is favoured over the ε position (Lys and hArg). Elongated aliphatic and hydrophobic residues in P1 decrease K_m, especially when aromatic groups are distant from the peptide backbone. This is evident by decreasing K_m values between nVal, Met, hPhe, Bpa, Glu(Bzl), and nLeu(o-Bzl). This tendency was also observed for CatC and DPAP1 and might suggest the presence of a distal binding pocket, potentially an exosite, since P1 residues are usually solvent exposed in clan CA proteases.

Not-surprisingly, variation in P2 residues has a bigger influence on K_m than P1, with Leu and nVal being optimal P2 residues for DPAP3. Interestingly, β-branched amino acids are not optimal for DPAP3 as can be observed by a decrease in K_m between Val and nVal or Ile and nLeu. However, the γ-branched amino acid Leu is well tolerated. Aliphatic P2 side chains that extend to the δ position (Met and nLeu) have higher K_m values than slightly shorter ones (Leu and nVal) but also higher k_{cat} values. Overall, combining optimal P1 (Arg and nLeu(o-Bzl)) and P2 (nVal and Leu) residues generally results in much improved k_{cat}/K_m values (Table 1).

Interestingly, although phenyl- and indanyl-glycine (Phg and Igl, respectively) in P2, or Bpa in P1 are not the preferred amino acids at these positions, these non-natural residues are structurally very different from natural amino acids and are turned over quite efficiently by rDPAP3 when combined with optimal P1 or P2 residues, respectively, i.e. Leu-Bpa-ACC or Phg-nLeu(o-Bzl). Finally, the optimal substrate for DPAP1, hPro-hPhe-ACC[32], is a very poorly turned over by rDPAP3 (>200-fold difference in k_{cat}/K_m). We think that these substrates containing

non-natural amino acids could be used as specific tools to measure DPAP1 or DPAP3 activity in biological samples, i.e. parasite lysates or live parasites, an application we are currently investigating.

Finally, our studies show that substrates with aromatic P2 residues are poorly cleaved by rDPAP3, i.e. 100 to 1000-fold lower k_{cat}/K_m compared to optimal substrates. This is surprising since vinyl sulfone inhibitors containing aromatic P2 residues (Tyr(NO_2), Tyr, Trp) are potent and selective DPAP3 inhibitors[19,26]. To better understand the discrepancy between substrates and inhibitors, we measured the kinetics of inactivation of rDPAP3 by the previously published vinyl sulfone inhibitor library[25,26].

DPAP3 Inhibitor Specificity.

The time- and concentration-dependent inactivation of rDPAP3 by the P2 library of vinyl sulfone inhibitors containing a fixed P1 hPhe residue was measured using a continuous assay at sub-saturating concentrations of a fluorogenic substrate (0.25 x K_m). The inhibition constants obtained are reported in Fig 2A and Table 2 and the individual fits for each inhibitor shown in Fig. S2.

For most compounds, the mechanism of DPAP3 inhibition was consistent with a two-step irreversible inhibition model (Eq. 3, Fig. 2B) except for two exceptions: a few inhibitors bound very poorly and only k_{inact}/K_i values could be obtained, i.e. no saturation was achieved in the k_{obs} *vs*. [I] graph (Fig. 2C). The other exception was the inhibitor with an amino-methyl-benzyl (Amb) group in P2, where no evidence of irreversible inhibition was observed (Fig 2D). This is probably due to the fact that this extended and rigid amino acid might prevent proper positioning of the vinyl sulfone group in the active site of DPAP3 to allow covalent modification of the catalytic Cys.

Overall, changes in P2 do not have a big influence in k_{inact} with the exceptions of Asn, Phe(Me), and Tyr(NO_2), which significantly increase k_{inact}. Intriguingly, substrates containing the latter two P2 residues were the only substrates with a P2 aromatic residue that could be cleaved by DPAP3 with $k_{cat}/K_m > 2{,}000\ M^{-1}s^{-1}$ (Table 1). In terms of K_i, we observed some SAR similarities between substrates and inhibitors: rDPAP3 does not bind inhibitors with an N-terminal basic

residue (Arg or Lys), but it is strongly inhibited (K_i < 25 nM) by aliphatic residues (Leu, nLeu, hAla, Val or nVal). However, we observed very potent inhibition of DPAP3 with aromatic residues in P2 such as Phe, Tyr or Trp ($k_{inact}/K_i \geq$ 60,000 $M^{-1}s^{-1}$). Substrates with these P2 residues show relatively poor substrate turnover ($k_{cat}/K_m \leq$ 2,000 $M^{-1}s^{-1}$).

The k_{inact}/K_i values obtained for DPAP3 with this inhibitor library was compared with k_{obs} values previously obtained for DPAP1 after incubating parasite lysates for 30 min with a dose response of inhibitor and using a DPAP1-selective substrate to measure residual DPAP1 activity [25]. As shown in Fig. 3E, inhibitors with P2 aromatic residues provide specificity towards DPAP3, while the inhibitor with a P2 Pro is the only compound in the library that is selective for DPAP1. Inhibitors containing short aliphatic residues such as Val or hAla are very potent inhibitors for both proteases.

Development of DPAP1 and DPAP3-selective inhibitors

We then synthesized a few extra inhibitors to see whether the optimal nLeu(O-Bzl) P1 residue identified from the substrate screen will increase the potency and specificity of inhibitors towards DPAP1 or DPAP3. We selected P2 residues that we predicted would provide specificity towards DPAP1 (Pro and hPro) or DPAP3 (aromatic residues: Tyr, Trp, Igl and 2Nal). The inhibition constants of these compounds were determined for DPAP1, DPAP3, and CatC (Table 3). The major structural difference between these compounds and the inhibitor library is that they have a phenyl group in P' instead of a long aliphatic linker. This change usually increases the potency of compounds by 2.5 to 32-fold, except in the context of a P2 Trp where it drops by 2.5-fold (Tables 2 and 3).

Compared to hPhe, P1 nLeu(O-Bzl) usually decreases k_{inact}/K_i value for rDPAP3 by 7 to 10-fold except in the context of a P2 Trp where it increases it by 24-fold (Table 3). These differences are mainly due to changes in K_i rather than k_{inact} and likely reflect interdependence between the S1 and S2 pockets of rDPAP3. However, in the case of DPAP1 and Cat C, replacement of P1 hPhe with nLeu(O-Bzl) usually decreases K_i. Because of this P1-P2 interdependence, the most potent inhibitors for DPAP3 are either a combination of P2 Tyr(NO_2) and P1 hPhe, i.e. SAK1, or P2 Trp and P1 nLeu(O-Bzl) resulting in k_{inact}/K_i values close to 10^6 $M^{-1}s^{-1}$. This very high second order rate constant is mainly driven by very low K_i values (< 10 nM). While these

two inhibitors and Igl-hPhe-VS show more than a 100-fold selectivity for DPAP3 over DPAP1, only SAK1 is highly selective for DPAP3 compared to CatC.

SAK2 is 100-fold more selective towards DPAP1 than DPAP3, but only shows a 10-fold selectivity for DPAP1 compared to CatC. While replacing the P2 Pro of SAK2 with hPro increases the potency of the inhibitors towards DPAP1, this also results in some loss of specificity (Table 3 and Fig. S3). That said, it is important to mention that the potency of SAK2 towards DPAP1 was increased 7-fold (from $0.5 \cdot 10^6$ to $3.6 \cdot 10^6$ $M^{-1}s^{-1}$) by using optimal P1 (nLeu(o-Bzl)) and P2 (hPro) residues that were identified by screening the substrate library[32], and makes hPro-nLeu(o-Bzl)-VS the most potent DPAP1 inhibitor identified so far[25,26,49].

Testing inhibitors specificity in live parasites.

We then decided to test our DPAP1 or DPAP3 specific inhibitors in live parasites using a competition assay with the FY01 ABP. Inhibitors with a P2 Pro or hPro are equally potent and inhibit DPAP1 at mid nanomolar concentrations. However, the P2 Pro makes the inhibitor much more selective by preventing inhibition of the falcipains (Fig. 4). Compounds having a P2 Trp or Tyr(NO_2) are highly specific for DPAP3 in intact parasites (Fig. 4). Interestingly, while SAK1 and Trp-nLeu(o-Bzl)-VS are equally potent against rDPAP3 (Table 3), the former is about 10-fold more potent in live parasites. Surprisingly, Trp-hPG-VS is by far the most potent DPAP3 inhibitor in intact parasites despite being 5 to 100-fold less potent than Trp-nLeu(o-Bzl)-VS or Trp-hPhe-VS against rDPAP3 (see k_{inact}/K_i values in Table 3). This suggests either that this compound is metabolically more table and/or that decreasing the hydrophobicity of the P1 residue enhances the cell permeability of the compound. Indeed, to reach DPAP3 compounds need to cross four membranes: the RBC, parasitophorous vacuole, and parasite membranes, plus the membrane of the apical organelle where DPAP3 resides[19]. (The parasitophorous vacuole is a membrane bound structure within which the parasite growth and multiply isolated from the RBC cytosol.) It is also possible that the apparent increased potency of Trp-hPG-VS in live parasites might be due its accumulation into the DPAP3 acidic organelle via protonation of its free amine.

DISCUSSION

Positional scanning substrate libraries have been used over the last 20 years[27-29] to determine the specificity of proteases and guide the synthesis of inhibitors. Indeed, vinyl sulfone inhibitors containing P1 and P2 residues identified as optimal for DPAP1 or DPAP3 substrates also show very potent inhibition. However, our studies clearly identified differences in specificity between substrates and inhibitors and indicate that potent inhibitors can also be developed based on the structure of poor substrates. In particular, we show that while aliphatic residues in the P2 position are optimal as DPAP3 substrates and inhibitors, substrates with aromatic P2 residues are poorly cleaved by DPAP3 but yield equally potent and much more selective inhibitors than those obtained from optimal substrate sequences (Fig. 3E and Tables 2 and 3). There are multiple reasons that can account for this discrepancy in specificity between substrates and inhibitors:

i. Although the substrate and inhibitor libraries used here have equivalent P1 and P2 residues, the structural features that bind into the S' pockets are quite different. Therefore, if the specificity of a protease shows interdependence between its prime and non-prime binding pockets, it might explain the difference in specificity. Indeed, we observed a 50-fold increase in k_{cat} between the Phe-Arg-ACC and Phe-Arg-βNA substrates, which only differ in the structure of the fluorphore that binds in the P1' binding pocket (Table 1). Therefore, within the context of a natural substrate that occupies all the prime side binding pockets, it is likely that DPAP3 will efficiently cleave substrates containing N-terminal aromatic residues.

ii. The position of the inhibitor electrophilic warhead within the active site might differ from that of the scissile bond in a substrate, especially in terms of distance and orientation relative to the catalytic Cys. This positioning might also be differently affected by changes in the P1 and P2 residues.

iii. Substrate turnover by Cys and Ser proteases requires two different chemical steps, i.e. nucleophilic attack of the peptide bond by the catalytic residue to form the acyl intermediate and release of the N-terminal product of proteolysis, and hydrolysis of the acyl intermediate by an activated water molecule to reconstitute the free enzyme and release the C-terminal

product of the reaction (Scheme 1). Therefore, substrate sequences that are poorly turned over because of a very slow acyl intermediate hydrolysis might still be very good covalent inhibitors. For example, a substrate that excludes the catalytic water from the active site upon formation of the acyl intermediate will be very poorly turned over.

$$\mathrm{E} + \mathrm{I} \underset{k_{\mathrm{off}}}{\overset{k_{\mathrm{on}}}{\rightleftarrows}} \mathrm{E{:}I} \xrightarrow{k_{\mathrm{inact}}} E - I$$

$$K_{\mathrm{i}} = \frac{k_{\mathrm{off}}}{k_{\mathrm{on}}}\ ;\ \frac{k_{\mathrm{inact}}}{K_{\mathrm{i}}} = \frac{k_{\mathrm{on}} \cdot k_{\mathrm{inact}}}{k_{\mathrm{off}}}$$

$$\mathrm{E} + \mathrm{S} \underset{k_{\mathrm{off}}}{\overset{k_{\mathrm{on}}}{\rightleftarrows}} \mathrm{E{:}S} \xrightarrow{k_{\mathrm{Ac}}} \mathrm{P_C} + \mathrm{E} - \mathrm{Ac} \xrightarrow{k_{\mathrm{Dac}}} \mathrm{P_N} + \mathrm{E}$$

$$k_{\mathrm{cat}} = \frac{k_{\mathrm{Ac}} \cdot k_{\mathrm{Dac}}}{k_{\mathrm{Ac}} + k_{\mathrm{Dac}}}\ ;\ K_{\mathrm{m}} = \frac{k_{\mathrm{Dac}} \cdot (k_{\mathrm{off}} + k_{\mathrm{Ac}})}{k_{\mathrm{on}} \cdot (k_{\mathrm{Ac}} + k_{\mathrm{Dac}})}\ ;\ \frac{k_{\mathrm{cat}}}{K_{\mathrm{m}}} = \frac{k_{\mathrm{on}} \cdot k_{\mathrm{Ac}}}{(k_{\mathrm{off}} + k_{\mathrm{Ac}})}$$

Scheme 1. Comparison between irreversible inhibition and substrate turnover kinetic constants. E, I, E:I and E-I represent free enzyme, inhibitor, inhibitor associated with the enzyme, and enzyme covalently modified by the inhibitor, respectively. S, E:S, E-Ac, P_C and P_N represent the substrate, the Michaelis Menten enzyme-substrate complex, the acyl intermediate, and the C- and N-terminal products of proteolysis, respectively; k_{on} and k_{off} the association and dissociation rate constant for substrate or inhibitor; and k_{Ac} and k_{Dac} the kinetic constants for formation of the acyl intermediate and its hydrolysis, respectively.

iv. Finally, the reaction mechanism between covalent inhibition and substrate turnover are quite different making k_{cat}, K_m, and k_{cat}/K_m not directly comparable with k_{inact}, K_i, and k_{inact}/K_i (Scheme 1). First, k_{cat}, K_m, and k_{cat}/K_m are empirical parameters obtained under steady state conditions while k_{inact}, K_i, and k_{inact}/K_i are real kinetic and thermodynamic constants that cannot be measured under steady state conditions since covalent inhibitors deplete the concentration of free enzyme over time. Second, k_{cat} might be equivalent to k_{inact} only if $k_{Ac} << k_{Dac}$, i.e. formation of the acyl intermediate is the rate limiting step; K_m might be equivalent to K_i only if $k_{Ac} << k_{off}$ and $k_{Ac} << k_{Dac}$; and k_{cat}/K_m might be equivalent to k_i/K_i only if $k_{off} >> k_{Ac}$. Although these conditions might be met for certain substrates, it is important to mentioned that the relative magnitudes of all these rate constants depend on the substrate sequence. For example, detailed pre-steady state kinetics and kinetic isotope effects studies on CatC have shown that the rate limiting step in the turnover of dipeptidic AMC substrates can be either formation of the acyl intermediate, its hydrolysis, or a contribution of both depending on the substrate sequence[50,51].

This study provides the first characterization of the specificity of DPAP3, a cysteine protease important for efficient invasion of RBCs by the malaria parasite[19]. Our study indicates that DPAP3 is a highly efficient proteolytic enzyme showing similar k_{cat} values than either DPAP1 or CatC when optimal substrates are used (Table 1). In general, DPAP3 has a narrower substrate specificity than either DPAP1 or CatC, and preferentially cleaves substrates with aliphatic residues at the N-terminus. Our study also shows very similar P1 specificity across all DPAPs, i.e. a strong preference for basic or long aromatic residues. DPAP3 was the only DPAP able to cleave some substrates with aromatic P2 residues (Tyr, Phe(Me), Phg), albeit with relatively low turnover rates. Surprisingly, vinyl sulfone inhibitors with aromatic residues are some of the most potent DPAP3 inhibitors and show very strong specificity for DPAP3 compared to DPAP1, CatC, or other malarial clan CA proteases, i.e. the falcipains. The previously described DPAP1 inhibitor SAK2 (Pro-hPhe-VS) show the best specificity for DPAP1 in live parasites. Although incorporating optimal P1 (nLeu(o-Bzl) and P2 (hPro) residues identified from substrate screen improves the potency of DPAP1 inhibitors both *in vitro* and in live parasites, this also results in a loss of specificity.

From a drug development point of view, our SAR studies indicate that inhibitors with short aliphatic P2 residues were able to potently inhibit both DPAPs (Fig. 3E) indicating that pan-DPAP inhibitors can easily been developed. Unfortunately, we did not identify any clear P1 or P2 residue that would discriminate malarial DPAPs from host CatC. Therefore, further studies are required to determine whether differences in specificity in the prime binding pockets can be exploited to develop parasite specific inhibitors.

That said, it is important to point that given the short-term treatment requirement for an antimalarial therapy (1-3 doses for 1-3 days), we think it is unlikely that inhibition of CatC would lead to adverse side effects. Firstly, highly specific DPAP inhibitors might not be necessary given that high levels (>95%) of sustained inhibition of CatC are required to see a decrease in the activity of serine proteases activated by CatC[52]. Secondly, no signs of toxicity were observed in phase I clinical trials of GSK2793660 CatC covalent inhibitor when volunteers were treated daily for 21 days, albeit some side effects such as plantar and palmar epithelial desquamation were observed in 90% of volunteers[17]. However, this side effect was not observed in volunteer that received a single dose of CatC inhibitor, or within the first week

of daily treatment. This adverse effect is likely due to on-target CatC inhibition since Papillon-Lefèvre Syndrome patients, who have inactivating point mutations in the *cathepsin C* gene, also suffer from skin lesions such as scaly skin or hyperkeratosis[53]. Finally, because malaria pathology is in part mediated through an uncontrolled inflammatory response due to the release of toxic materials from iRBCs, it is possible that inhibition of CatC might actually help control the inflammatory response in patients by decreasing the level of pro-inflammaroty serine proteases activity. Overall, the results of this clinical trial suggest that off-target inhibition of human CatC might not be an issue in the context of malaria treatment but might be problematic if DPAP inhibitors want to be used as prophylactic agents.

Acknowledgement

We would like to thank the Wellcome Trust and Royal Society for funding this research and E.D. and C.L. through the Sir Henry Dale Fellowship 099950. We would also like to thank Erasmus for funding L.E.V. and L.K. internship in Dr. Edgar Deu's laboratory.

Authors Contributions

E.D. performed most of experiments, supervised the work, and wrote the manuscript. F.Y. synthesized the inhibitor library and M.P. the substrate library. M.I.S. and K.G. synthesized inhibitors and substrates for this study, respectively, and S.A.K. the SAK2 inhibitor. C.L. prepared the plasmid for the expression or rDPAP3, L.E.V. expressed and purified rDPAP3, and L.K. tested the inhibitors in live parasites. M.B. and M.D. supervised the synthesis of inhibitors and susbtrates, respectively.

References

1. World Health Organization. World Malaria Report 2016. 1–186 (2017).
2. Bhatt, S. *et al.* The effect of malaria control on Plasmodium falciparum in Africa between 2000 and 2015. *Nature* **526,** 207–211 (2015).
3. Ranson, H. & Lissenden, N. Insecticide Resistance in African Anopheles Mosquitoes: A Worsening Situation that Needs Urgent Action to Maintain Malaria Control. *Trends in Parasitology* **32,** 187–196 (2016).
4. Ashley, E. A. *et al.* Spread of artemisinin resistance in Plasmodium falciparum malaria.

N. Engl. J. Med. **371,** 411–423 (2014).

5. Wells, T. N. C., Hooft van Huijsduijnen, R. & Van Voorhis, W. C. Malaria medicines: a glass half full? *Nat Rev Drug Discov* **14,** 424–442 (2015).
6. Bozdech, Z. *et al.* The Transcriptome of the Intraerythrocytic Developmental Cycle of Plasmodium falciparum. *PLoS Biol.* **1,** e5–16 (2003).
7. Young, J. A. *et al.* The Plasmodium falciparum sexual development transcriptome: a microarray analysis using ontology-based pattern identification. *Molecular & Biochemical Parasitology* **143,** 67–79 (2005).
8. GUTMANN, H. R. & FRUTON, J. S. On the proteolytic enzymes of animal tissues; an intracellular enzyme related to chymotrypsin. *Journal of Biological Chemistry* **174,** 851–858 (1948).
9. WIGGANS, D. S., WINITZ, M. & FRUTON, J. S. Action of cathepsin C on dipeptide esters. *Yale J Biol Med* **27,** 11–19 (1954).
10. McGuire, M. J., Lipsky, P. E. & Thiele, D. L. Generation of active myeloid and lymphoid granule serine proteases requires processing by the granule thiol protease dipeptidyl peptidase I. *Journal of Biological Chemistry* **268,** 2458–2467 (1993).
11. Kummer, J. A., Kamp, A. M., Citarella, F., Horrevoets, A. J. & Hack, C. E. Expression of human recombinant granzyme A zymogen and its activation by the cysteine proteinase cathepsin C. *Journal of Biological Chemistry* **271,** 9281–9286 (1996).
12. Pham, C. T. & Ley, T. J. Dipeptidyl peptidase I is required for the processing and activation of granzymes A and B in vivo. *Proc Natl Acad Sci USA* **96,** 8627–8632 (1999).
13. Adkison, A. M., Raptis, S. Z., Kelley, D. G. & Pham, C. T. N. Dipeptidyl peptidase I activates neutrophil-derived serine proteases and regulates the development of acute experimental arthritis. *J. Clin. Invest.* **109,** 363–371 (2002).
14. Guay, D. *et al.* Design and synthesis of dipeptidyl nitriles as potent, selective, and reversible inhibitors of cathepsin C. *Bioorganic & Medicinal Chemistry Letters* **19,** 5392–5396 (2009).
15. Lainé, D. *et al.* Discovery of novel cyanamide-based inhibitors of cathepsin C. *ACS Med Chem Lett* **2,** 142–147 (2011).
16. Furber, M. *et al.* Cathepsin C inhibitors: property optimization and identification of a clinical candidate. *J. Med. Chem.* **57,** 2357–2367 (2014).
17. Miller, B. E. *et al.* Epithelial desquamation observed in a phase I study of an oral

cathepsin C inhibitor (GSK2793660). *Br J Clin Pharmacol* **83,** 2813–2820 (2017).

18. Klemba, M., Gluzman, I. & Goldberg, D. E. A Plasmodium falciparum dipeptidyl aminopeptidase I participates in vacuolar hemoglobin degradation. *J. Biol. Chem.* **279,** 43000–43007 (2004).
19. Lehmann, C. *et al.* Plasmodium falciparum dipeptidyl aminopeptidase 3 activity is important for efficient erythrocyte invasion by the malaria parasite. *bioRxiv* 1–39 (2017). doi:10.1101/202812
20. Lin, J.-W. *et al.* Replication of Plasmodiumin reticulocytes can occur without hemozoin formation, resulting in chloroquine resistance. *J Exp Med* **212,** 893–903 (2015).
21. Capuccini, B. *et al.* Transcriptomic profiling of microglia reveals signatures of cell activation and immune response, during experimental cerebral malaria. *Nature Publishing Group* **6,** 39258 (2016).
22. Schwach, F. *et al.* PlasmoGEM, a database supporting a community resource for large-scale experimental genetics in malaria parasites. *Nucleic Acids Res.* **43,** D1176–82 (2015).
23. Suárez-Cortés, P. *et al.* Comparative Proteomics and Functional Analysis Reveal a Role of Plasmodium falciparum Osmiophilic Bodies in Malaria Parasite Transmission. *Mol. Cell Proteomics* **15,** 3243–3255 (2016).
24. Tanaka, T. Q. *et al.* Plasmodium dipeptidyl aminopeptidases as malaria transmission-blocking drug targets. *Antimicrob. Agents Chemother.* **57,** 4645–4652 (2013).
25. Deu, E. *et al.* Functional Studies of Plasmodium falciparum Dipeptidyl Aminopeptidase I Using Small Molecule Inhibitors and Active Site Probes. *Chemistry & Biology* **17,** 808–819 (2010).
26. Arastu-Kapur, S. *et al.* Identification of proteases that regulate erythrocyte rupture by the malaria parasite Plasmodium falciparum. *Nat Chem Biol* **4,** 203–213 (2008).
27. Thornberry, N. A. *et al.* A combinatorial approach defines specificities of members of the caspase family and granzyme B. Functional relationships established for key mediators of apoptosis. *Journal of Biological Chemistry* **272,** 17907–17911 (1997).
28. Rano, T. A. *et al.* A combinatorial approach for determining protease specificities: application to interleukin-1beta converting enzyme (ICE). *Chemistry & Biology* **4,** 149–155 (1997).
29. Harris, J. L. *et al.* Rapid and general profiling of protease specificity by using

combinatorial fluorogenic substrate libraries. *Proc Natl Acad Sci USA* **97,** 7754–7759 (2000).

30. Drag, M., Bogyo, M., Ellman, J. A. & Salvesen, G. S. Aminopeptidase fingerprints, an integrated approach for identification of good substrates and optimal inhibitors. *J. Biol. Chem.* **285,** 3310–3318 (2010).
31. Poreba, M. *et al.* Fingerprinting the Substrate Specificity of M1 and M17 Aminopeptidases of Human Malaria, Plasmodium falciparum. *PLoS ONE* **7,** e31938–8 (2012).
32. Poreba, M. *et al.* Unnatural amino acids increase activity and specificity of synthetic substrates for human and malarial cathepsin C. *Amino Acids* **46,** 931–943 (2014).
33. Nazif, T. & Bogyo, M. Global analysis of proteasomal substrate specificity using positional-scanning libraries of covalent inhibitors. *Proc Natl Acad Sci USA* **98,** 2967–2972 (2001).
34. Greenbaum, D. C. *et al.* Small molecule affinity fingerprinting. A tool for enzyme family subclassification, target identification, and inhibitor design. *Chemistry & Biology* **9,** 1085–1094 (2002).
35. Kasperkiewicz, P. *et al.* Design of ultrasensitive probes for human neutrophil elastase through hybrid combinatorial substrate library profiling. *Proc. Natl. Acad. Sci. U.S.A.* **111,** 2518–2523 (2014).
36. Kasperkiewicz, P., Poreba, M., Groborz, K. & Drag, M. Emerging challenges in the design of selective substrates, inhibitors and activity-based probes for indistinguishable proteases. *FEBS J.* **284,** 1518–1539 (2017).
37. Poreba, M. *et al.* Unnatural amino acids increase activity and specificity of synthetic substrates for human and malarial cathepsin C. *Amino Acids* **46,** 931–943 (2014).
38. Wang, F. *et al.* Biochemical characterization of Plasmodium falciparum dipeptidyl aminopeptidase 1. *Molecular & Biochemical Parasitology* **175,** 10–20 (2011).
39. Poreba, M., Szalek, A., Kasperkiewicz, P. & Drag, M. Positional scanning substrate combinatorial library (PS-SCL) approach to define caspase substrate specificity. *Methods Mol. Biol.* **1133,** 41–59 (2014).
40. Yang, P.-Y., Wang, M., He, C. Y. & Yao, S. Q. Proteomic profiling and potential cellular target identification of K11777, a clinical cysteine protease inhibitor, in Trypanosoma brucei. *Chem. Commun. (Camb.)* **48,** 835–837 (2012).

41. Sanman, L. E. & Bogyo, M. Activity-Based Profiling of Proteases. *Annu. Rev. Biochem.* **83,** 249–273 (2014).

42. Yuan, F., Verhelst, S. H. L., Blum, G., Coussens, L. M. & Bogyo, M. A selective activity-based probe for the papain family cysteine protease dipeptidyl peptidase I/cathepsin C. *J. Am. Chem. Soc.* **128,** 5616–5617 (2006).

43. Morrison, J. F. & Walsh, C. T. The behavior and significance of slow-binding enzyme inhibitors. *Adv. Enzymol. Relat. Areas Mol. Biol.* **61,** 201–301 (1988).

44. Deu, E., Yang, Z., Wang, F., Klemba, M. & Bogyo, M. Use of activity-based probes to develop high throughput screening assays that can be performed in complex cell extracts. *PLoS ONE* **5,** e11985 (2010).

45. Sijwali, P. S., Koo, J., Singh, N. & Rosenthal, P. J. Gene disruptions demonstrate independent roles for the four falcipain cysteine proteases of Plasmodium falciparum. *Molecular & Biochemical Parasitology* **150,** 96–106 (2006).

46. Sijwali, P. S. *et al.* Plasmodium falciparum cysteine protease falcipain-1 is not essential in erythrocytic stage malaria parasites. *Proc Natl Acad Sci USA* **101,** 8721–8726 (2004).

47. Greenbaum, D. C. *et al.* A role for the protease falcipain 1 in host cell invasion by the human malaria parasite. *Science* **298,** 2002–2006 (2002).

48. Collins, C. R. *et al.* Malaria parasite cGMP-dependent protein kinase regulates blood stage merozoite secretory organelle discharge and egress. *PLoS Pathog* **9,** e1003344 (2013).

49. Mahajan, S. S. *et al.* A fragmenting hybrid approach for targeted delivery of multiple therapeutic agents to the malaria parasite. *ChemMedChem* **6,** 415–419 (2011).

50. Schneck, J. L. *et al.* Chemical mechanism of a cysteine protease, cathepsin C, as revealed by integration of both steady-state and pre-steady-state solvent kinetic isotope effects. *Biochemistry* **47,** 8697–8710 (2008).

51. Rubach, J. K. *et al.* The amino-acid substituents of dipeptide substrates of cathepsin C can determine the rate-limiting steps of catalysis. *Biochemistry* **51,** 7551–7568 (2012).

52. Methot, N. *et al.* In vivo inhibition of serine protease processing requires a high fractional inhibition of cathepsin C. *Mol. Pharmacol.* **73,** 1857–1865 (2008).

53. Haneke, E. The Papillon-Lefèvre syndrome: keratosis palmoplantaris with periodontopathy. Report of a case and review of the cases in the literature. *Hum. Genet.* **51,** 1–35 (1979).

Table1: Steady-state Michaelis Menten Parameters for rDPAP3.				
Substrate	N	k_{cat} (s^{-1})	K_m (μM)	$k_{cat}/K_m \cdot 10^{-3}$ ($M^{-1}s^{-1}$)
Met-His-ACC	4	0.23 ± 0.02	42 ± 10	5.4 ± 1
Met-nVal-ACC	4	0.54 ± 0.04	43 ± 5	13 ± 1
Met-hPhe-ACC	4	0.5 ± 0.02	20 ± 2	24 ± 2
Met-Met-ACC	4	0.54 ± 0.02	21 ± 2	26 ± 1
Met-Lys-ACC	4	1.00 ± 0.04	34 ± 2	29 ± 1
Met-Bpa-ACC	3	0.48 ± 0.04	14 ± 3	34 ± 4
Met-hArg-ACC	4	0.92 ± 0.02	27 ± 2	35 ± 1
Met-Arg-ACC	4	1.26 ± 0.06	31 ± 3	41 ± 2
Met-Glu(Bzl)-ACC	4	0.56 ± 0.04	13 ± 2	46 ± 6
Met-Arg(NO_2)-ACC	4	1.90 ± 0.08	23 ± 2	84 ± 4
Met-nLeu(o-Bzl)-ACC	10	1.66 ± 0.02	8.8 ± 0.4	186 ± 6
hPro-hPhe-ACC[1]	3	0.007 ± 0.001	26 ± 6	0.30 ± 0.04
Trp-hPhe-ACC	3	N.S.	N.S.	1.2 ± 0.2
Phe-hPhe-ACC	3	0.032 ± 0.008	20 ± 8	1.6 ± 0.2
Igl-hPhe-ACC	3	0.044 ± 0.004	4.7 ± 0.9	9.4 ± 1
hAla-hPhe-ACC	3	0.0014 ± 0.002	14.7 ± 0.8	9.8 ± 1
Ile-hPhe-ACC	4	0.12 ± 0.01	12 ± 3	10 ± 1
Phg-hPhe-ACC	4	0.110 ± 0.004	10 ± 1	11 ± 1
Phe(Me)-hPhe-ACC	3	0.072 ± 0.004	6 ± 1	12 ± 1
Tyr(NO_2)-hPhe-ACC	3	0.134 ± 0.002	9.9 ± 0.4	13.6 ± 0.4
Val-hPhe-ACC	3	0.24 ± 0.04	14 ± 4	18 ± 2
nLeu-hPhe-ACC	3	0.28 ± 0.02	5.9 ± 1.3	46 ± 6
nVal-hPhe-ACC	4	0.164 ± 0.005	1.30 ± 0.08	128 ± 6
Leu-hPhe-ACC	3	0.100 ± 0.002	0.50 ± 0.03	210 ± 10
Phg-nLeu(o-Bzl)-ACC	8	0.80 ± 0.02	7.8 ± 0.8	102 ± 6
Leu-nLeu(o-Bzl)-ACC	5	0.308 ± 0.006	0.5 ± 0.1	640 ± 100
nVal-nLeu(o-Bzl)-ACC	8	1.28 ± 0.02	1.4 ± 0.1	920 ± 60
Leu-Bpa-ACC	4	0.170 ± 0.004	0.61 ± 0.06	280 ± 20
Phe-Arg-ACC	4	0.018 ± 0.006	20 ± 10	0.9 ± 0.2
Pro-Arg-AMC[2]	3	0.102 ± 0.004	88 ± 5	1.16 ± 0.04
Val-Arg-ACC[3]	3	1.08 ± 0.06	63 ± 5	17.0 ± 0.4
Leu-Arg-ACC	8	0.330 ± 0.006	1.8 ± 0.2	185 ± 15
nVal-Arg-ACC	8	0.346 ± 0.004	0.72 ± 0.05	480 ± 30
Phe-Arg-BNA	4	0.96 ± 0.04	51 ± 5	19 ± 1

[1]For DPAP1, k_{cat} = 0.22 ± 0.004 s^{-1}, K_m = 0.67 ± 0.14 μM and k_{cat}/K_m = 320,000 ± 50,000 $M^{-1}s^{-1}$; for CatC, k_{cat} = 10.8 ± 0.2 s^{-1}, K_m = 91 ± 5 μM and k_{cat}/K_m = 116,000 ± 11,000 $M^{-1}s^{-1}$.[32]
[2]For DPAP1, k_{cat} = 6.2 ± 0.4 s^{-1}, K_m = 84 ± 9 μM and k_{cat}/K_m = 74,000 ±2000 $M^{-1}s^{-1}$; for CatC, k_{cat} = 490 ± 10 s^{-1}, K_m = 130 ± 10 μM and k_{cat}/K_m = 3,600,000 ±300,000 $M^{-1}s^{-1}$.[38]
[3]For DPAP1, k_{cat} = 3.5 ± 0.1 s^{-1}, K_m = 21 ± 2 μM and k_{cat}/K_m = 170,000 ± 10,000 $M^{-1}s^{-1}$; for CatC, k_{cat} = 180 ± 10 s^{-1}, K_m= 51 ± 8 μM and k_{cat}/K_m =3,600,000 ± 300,000 $M^{-1}s^{-1}$.[38]

Table 2: Inhibition constants for VS inhibitors library					
ID[25]	P2	P2 AA structure	$k_{inact} \cdot 10^{-3}$ (s^{-1})	K_i (nM)	$k_{inact}/K_i \cdot 10^{-3}$ ($M^{-1}s^{-1}$)
A1	Gly		4.2 ± 0.3	3,300 ± 700	1.3 ± 0.2
A2	Ala		2.4 ± 0.1	88 ± 13	27 ± 3
D4	Acpc		3.2 ± 0.1	47,000 ± 3,000	0.0677 ± 0.0001
D5	hAla		2.2 ± 0.3	13.5 ± 6	166 ± 50
D6	Aib		N.S.	N.S.	0.0363 ± 0.0006
F1	Val		3.2 ± 0.2	5.7 ± 1	554 ± 84
F2	Ile	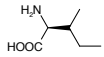	3.4 ± 0.4	23 ± 9	148 ± 44
D8	Cba	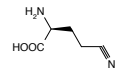	2.5 ± 0.1	420 ± 30	17.2 ± 2.5
E3	Thr	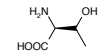	2.0 ± 0.1	36 ± 8	55 ± 10
A4	Asn	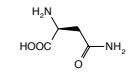	7.4 ± 0.8	2,100 ± 1000	3.5 ± 1.4
A7	Gln	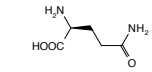	2.8 ± 0.1	62 ± 13	46 ± 8
A5	Asp	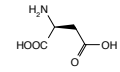	2.9 ± 0.2	1,900 ± 400	1.5 ± 0.2
A8	Glu	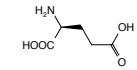	2.7 ± 0.1	51 ± 8	53 ± 6
A9	His	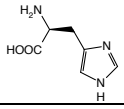	3.1 ± 0.3	110 ± 35	29 ± 8
A11	Lys	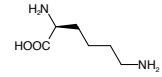	N.S.	N.S.	0.020 ± 0.001
A3	Arg	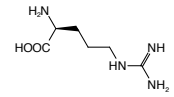	N.S.	N.S.	0.065 ± 0.006
E4	Phg	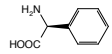	N.S.	N.S.	0.0357 ± 0.0007
D1	2fa	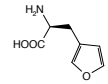	3.8 ± 0.3	39 ± 10	97 ± 18
D2	2ta	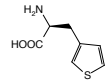	3.4 ± 0.3	29 ± 7	118 ± 23
E11	Cha	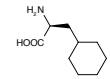	2.2 ± 0.1	29 ± 5	78 ± 12
A12	Phe	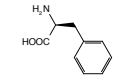	2.07 ± 0.07	37 ± 4	60 ± 5
D11	Phe(Me)	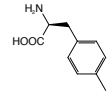	14 ± 3	33,000 ± 9,000	0.42 ± 0.03

D9	I-Phe	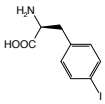	3.8 ± 0.3	110 ± 30	36 ± 10
D10	Phe(NH2)	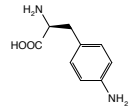	3.1 ± 0.2	39 ± 7	80 ± 12
E1	Tyr	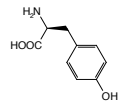	2.2 ± 0.7	12.7 ± 1.5	172 ± 16
D12	Tyr(NO_2)	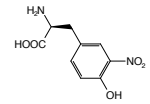	7.2 ± 0.9	251 ± 37	28.8 ± 0.8
E9	hPhe	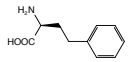	2.36 ± 0.08	312 ± 34	7.6 ± 0.7
E2	Trp	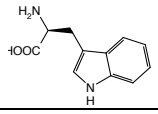	2.5 ± 0.1	30 ± 6	84 ± 14
E12	Igl	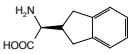	2.7 ± 0.2	86 ± 18	32 ± 6
E10	2Nal	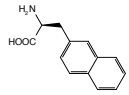	3.7 ± 0.3	7,100 ± 1,000	0.51 ± 0.04
E8	Bip	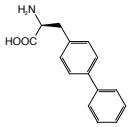	N.S.	N.S.	0.0314 ± 0.0004
E5	Inp		5.2 ± 0.4	65,000 ± 800	0.079 ± 0.004
E6	Amc	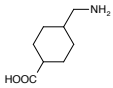	5.7 ± 0.3	75,000 ± 7,000	0.076 ± 0.003
D3	3Abz		3.4 ± 0.4	3,100 ± 600	1.1 ± 0.1
E7	Amb	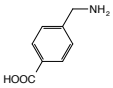	N/A	3,200 ± 1000	N/A
N.S. No saturation, only k_{inact}/K_i could be obtained. N/A, no time dependent inactivation was observed, data consistent with reversible inhibition.					

Table 3: Inhibition constants for optimal VS inhibitors

Name	P1	P2	DPAP3			DPAP1			CatC			Specificity Ratio[a]		
			$k_{inact} \cdot 10^{-3}$ (s^{-1})	K_i (nM)	$k_{inact}/K_i \cdot 10^{-3}$ ($M^{-1}s^{-1}$)	$k_{inact} \cdot 10^{-3}$ (s^{-1})	K_i (nM)	$k_{inact}/K_i \cdot 10^{-3}$ ($M^{-1}s^{-1}$)	$k_{inact} \cdot 10^{-3}$ (s^{-1})	K_i (nM)	$k_{inact}/K_i \cdot 10^{-3}$ ($M^{-1}s^{-1}$)	DPAP1/ DPAP3	DPAP1/ CatC	DPAP3/ CatC
SAK2	hPhe	Pro	3.5 ± 0.2	860 ± 100	4.1 ± 0.3	2.1 ± 0.2	4.6 ± 0.7	470 ± 35	1.45 ± 0.07	34 ± 5	42 ± 5	**115**	11	0.10
MSED42	hPhe	hPro	2.1 ± 0.1	30 ± 7	69 ± 13	4.8 ± 0.6	3.9 ± 1.5	1230 ± 400	1.67 ± 0.08	22 ± 3	76 ± 0.8	18	16	0.91
MSED55	nLeu(o-Bzl)	hPro	2.0 ± 0.8	39 ± 6	53 ± 6.5	2.9 ± 0.3	0.8 ± 0.2	3560 ± 150	1.67 ± 0.03	11.2 ± 0.6	150 ± 6	68	24	0.35
SAK1	hPhe	Tyr(NO_2)	2.26 ± 0.05	2.4 ± 0.2	950 ± 740	3.8 ± 1	25000 ± 14000	0.15 ± 0.05	3.2 ± 0.6	58000 ± 20000	0.054 ± 0.008	**0.00016**	2.8	**17600**
MSED58	nLeu(o-Bzl)	Tyr(NO_2)	2.7 ± 0.2	80 ± 15	34 ± 5	2.6 ± 0.3	2400 ± 900	1.1 ± 0.3	2.9 ± 0.2	7700 ± 1400	0.38 ± 0.05	0.032	2.9	89
MSED43	hPhe	2Nal	2.59 ± 0.07	254 ± 16	10.2 ± 0.5	6.7 ± 0.2	33000 ± 2000	0.2 ± 0.005	3.7 ± 0.2	4000 ± 700	0.9 ± 0.1	0.02	0.22	11
MSED56	nLeu(o-Bzl)	2Nal	6.0 ± 0.7	4170 ± 100	1.4 ± 0.2	5.0 ± 1.7	27000 ± 16000	0.19 ± 0.05	2.4 ± 0.6	1740 ± 140	1.37 ± 0.09	0.14	0.14	1.0
MSED44	hPhe	Igl	2.1 ± 0.7	10 ± 1	205 ± 22	2.7 ± 0.1	5400 ± 500	0.50 ± 0.03	5.8 ± 0.3	320 ± 65	18 ± 3	**0.0024**	0.028	11.4
MSED57	nLeu(o-Bzl)	Igl	5.6 ± 0.4	240 ± 40	23.5 ± 3	4.1 ± 0.2	4800 ± 500	0.86 ± 0.05	1.48 ± 0.06	11 ± 2	135 ± 14	0.037	**0.0064**	0.17
MSED21	hPG	*L*-Trp	3 ± 1	500 ± 240	6 ± 1	2.1 ± 0.2	2800 ± 450	0.74 ± 0.07	1.73 ± 0.03	28 ± 2	61 ± 4	0.12	0.012	0.10
WSAK	hPhe	*L*-Trp	3.3 ± 0.4	97 ± 20	34 ± 4	1.7 ± 0.1	540 ± 80	3.20 ± 0.3	2.2 ± 0.09	16 ± 3	131 ± 15	0.094	0.024	0.26
MSED68	nLeu(o-Bzl)	*L*-Trp	3.2 ± 0.3	4 ± 1	826 ± 193	2.2 ± 0.1	380 ± 60	5.8 ± 0.6	1.74 ± 0.03	4.9 ± 0.3	355 ± 18	**0.0070**	0.016	2.3
MSED67	hPhe	*D*-Trp	1.7 ± 0.6	8230 ± 4600	0.21 ± 0.06	2.7 ± 0.2	104800 ± 10000	0.026 ± 0.001	2.6 ± 0.1	4200 ± 600	0.62 ± 0.07	0.12	0.042	0.34
MSED71	nLeu(o-Bzl)	*D*-Trp	3.6 ± 0.2	7,600 ± 600	0.47 ± 0.01	5.5 ± 0.7	127000 ± 20000	0.044 ± 0.002	1.97 ± 0.06	1100 ± 100	1.7 ± 0.1	0.094	0.026	0.28

[a]Specificity ratio was calculated based on k_{inact}/K_i values; numbers highlighted in bold indicate more than 100-fold selectivity for the indicated enzymes.

FIGURE LEGENDS

Figure 1. Active site titration of rDPAP3 using activity-based probes.

(**A**) Labelling of purified rDPAP3 by FY01 in the presence or absence of SAK1. Our stock of rDPAP3 was diluted 20-fold in assay buffer, treated with DMSO or 1 μM SAK1 for 30 min, and labelled with FY01 for 1 h. Samples were run on an SDS-PAGE gel and DPAP3 labelling measured using a flatbed fluorescence scanner. (**B**) Calibration curve of free probe measured on the same SDS-PAGE gel as the one shown in A. (**C**) The fluorescence signal for rDPAP3 labelling and free probe was quantified using Image J, and the concentration of labelled rDPAP3 calculated based on the calibration curve.

Figure 2. DPAP3 substrate specificity.

(**A**) Structure of P1 and P2 substrate libraries. (**B**) Heat map comparing relative turnover rates for the different DPAPs at 1 μM substrate. For each enzyme and substrate turnover rates were normalized relative to the best natural amino acid in the variable position (dark green): Arg in P1 for all DPAPs; Met, Val, and Leu in P2 for CatC, DPAP1, and rDPAP3, respectively. Red indicates substrates that are turned over better than the best natural amino acid. White represent no activity, and grey substrates that were only tested on rDPAP3. (**C**) Structure of non-natural amino acids used in the substrate library. (**D**) Steady-state Michaelis Menten parameters for rDPAP3 determined for selected substrates.

Figure 3. DPAP3 inhibitor specificity.

(**A**) Inhibition constants determine for rDPAP3. The general structure of the inhibitors is shown below the graphs. White bars correspond to substrate for which only k_{inact}/K_i values could be determined. The grey bar corresponds to the only inhibitor that showed a reversible mechanism of inhibition, i.e. only a K_i value could be determined. (**B**) Representative data showing time-dependent inhibition of rDPAP3 by SAK1. Each progress curve (FU vs. time) was fitted to Eq. 4 to obtain k_{obs} values (top graph). These were then fitted to Eq. 5 to obtain k_{inact} and K_i. (**C**) Example of an inhibitor where no inhibitor saturation was observed (white bars in **A**). In this case, k_{obs} values were fitted to a linear model to obtain k_{inact}/K_i. (**D**) No time-dependence inhibition of rDPAP3 was observed with an inhibitor with a P2 Amb. Initial turnover rates (V_0) were fitted to a reversible binding model to obtain K_i. (**E**) Comparison of

k_{inact}/K_i obtain with rDPAP3 and k_{obs} values previously determined for DPAP1[25]. Large hydrophobic residues show selectivity for DPAP3 while Pro is the only amino acid that shows DPAP1 selectivity. Short aliphatic residues in P2 result in potent inhibition of both DPAPs.

Figure 4. Selective inhibition of DPAP1 or DPAP3 in live parasites.

Intact mature schizonts were pre-treated for 30 min with a dose response of inhibitor followed by 1 h treatment with FY01 to label the residual level of DPAPs and falcipains activity. Fluorescents bands corresponding to the different cysteine proteases labelled with the probe are indicated by arrow. An apparent IC_{50} value for each protease and inhibitor is shown next to each gel. Inhibitors with Pro or hPro in P2 are highly selective for DPAP1, and those with Tyr(NO_2) or *L*-Trp are specific for DPAP3. Note that control inhibitors containing *D*-Trp are more than 1000-fold less potent than those with *L*-Trp.

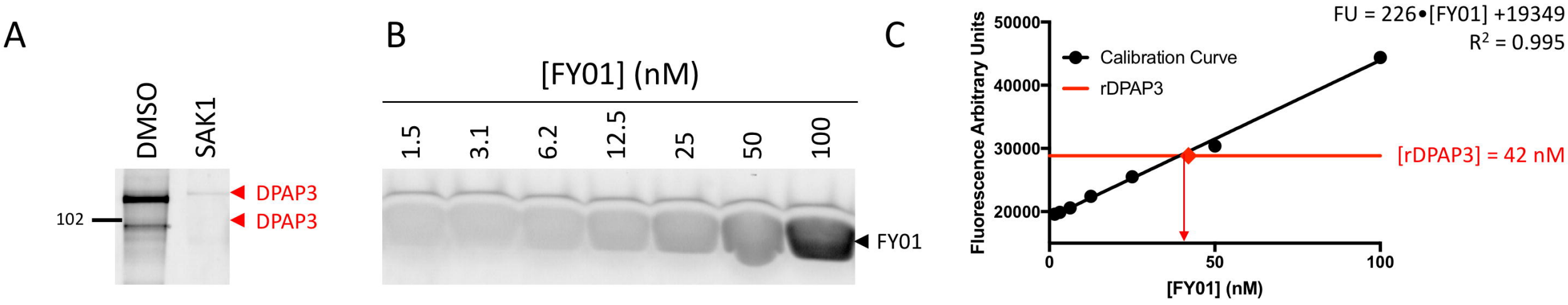
A
DMSO
SAK1
102
DPAP3
DPAP3
B
[FY01] (nM)
1.5
3.1
6.2
12.5
25
50
100
FY01
C
FU = 226•[FY01] +19349
R² = 0.995
Calibration Curve
rDPAP3
[rDPAP3] = 42 nM
Fluorescence Arbitrary Units
50000
40000
30000
20000
0
50
100
[FY01] (nM)

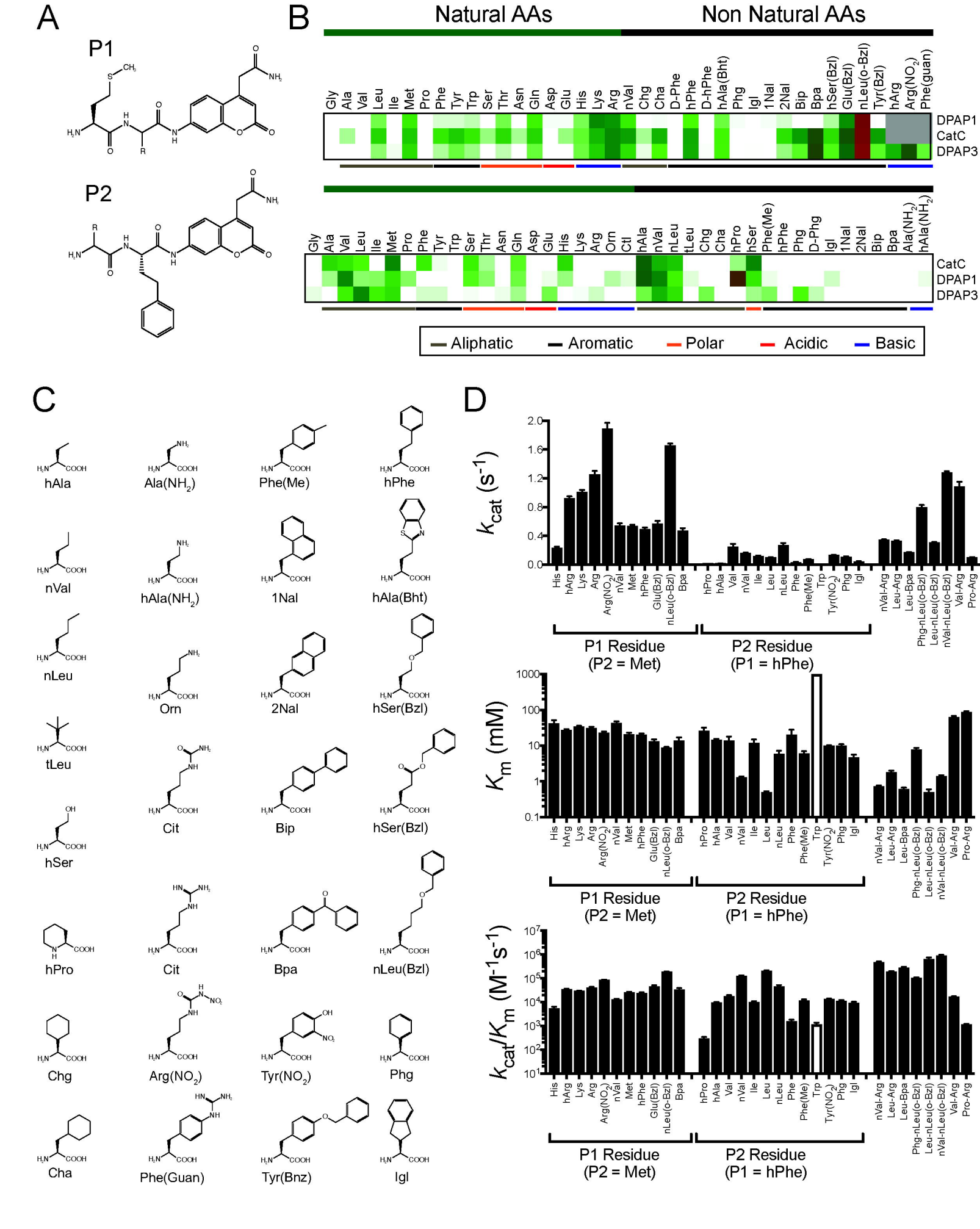
A
P1
P2
B
Natural AAs
Non Natural AAs
Gly Ala Val Leu Ile Met Pro Phe Tyr Trp Ser Thr Asn Gln Asp Glu His Lys Arg nVal Chg Cha D-Phe hPhe D-hPhe hAla(Bht) Phg Igl 1Nal 2Nal Bip Bpa hSer(Bzl) Glu(Bzl) nLeu(o-Bzl) Tyr(Bzl) hArg Arg(NO2) Phe(guan)
DPAP1
CatC
DPAP3
Gly Ala Val Leu Ile Met Pro Phe Tyr Trp Ser Thr Asn Gln Asp Glu His Lys Arg Orn Ctl hAla nVal nLeu tLeu Chg Cha hPro hSer Phe(Me) hPhe Phg D-Phg Igl 1Nal 2Nal Bip Bpa Ala(NH2) hAla(NH2)
CatC
DPAP1
DPAP3
Aliphatic
Aromatic
Polar
Acidic
Basic
C
hAla
Ala(NH2)
Phe(Me)
hPhe
nVal
hAla(NH2)
1Nal
hAla(Bht)
nLeu
Orn
2Nal
hSer(Bzl)
tLeu
Cit
Bip
hSer(Bzl)
hSer
hPro
Cit
Bpa
nLeu(Bzl)
Chg
Arg(NO2)
Tyr(NO2)
Phg
Cha
Phe(Guan)
Tyr(Bnz)
Igl
D
kcat (s-1)
Km (mM)
kcat/Km (M-1s-1)
His hArg Lys Arg Arg(NO2) nVal Met hPhe Glu(Bzl) nLeu(o-Bzl) Bpa
hPro hAla Val nVal Ile Leu nLeu Phe Phe(Me) Trp Tyr(NO2) Phg Igl
nVal-Arg Leu-Arg Leu-Bpa Phg-nLeu(o-Bzl) Leu-nLeu(o-Bzl) nVal-nLeu(o-Bzl) Val-Arg Pro-Arg
P1 Residue
(P2 = Met)
P2 Residue
(P1 = hPhe)

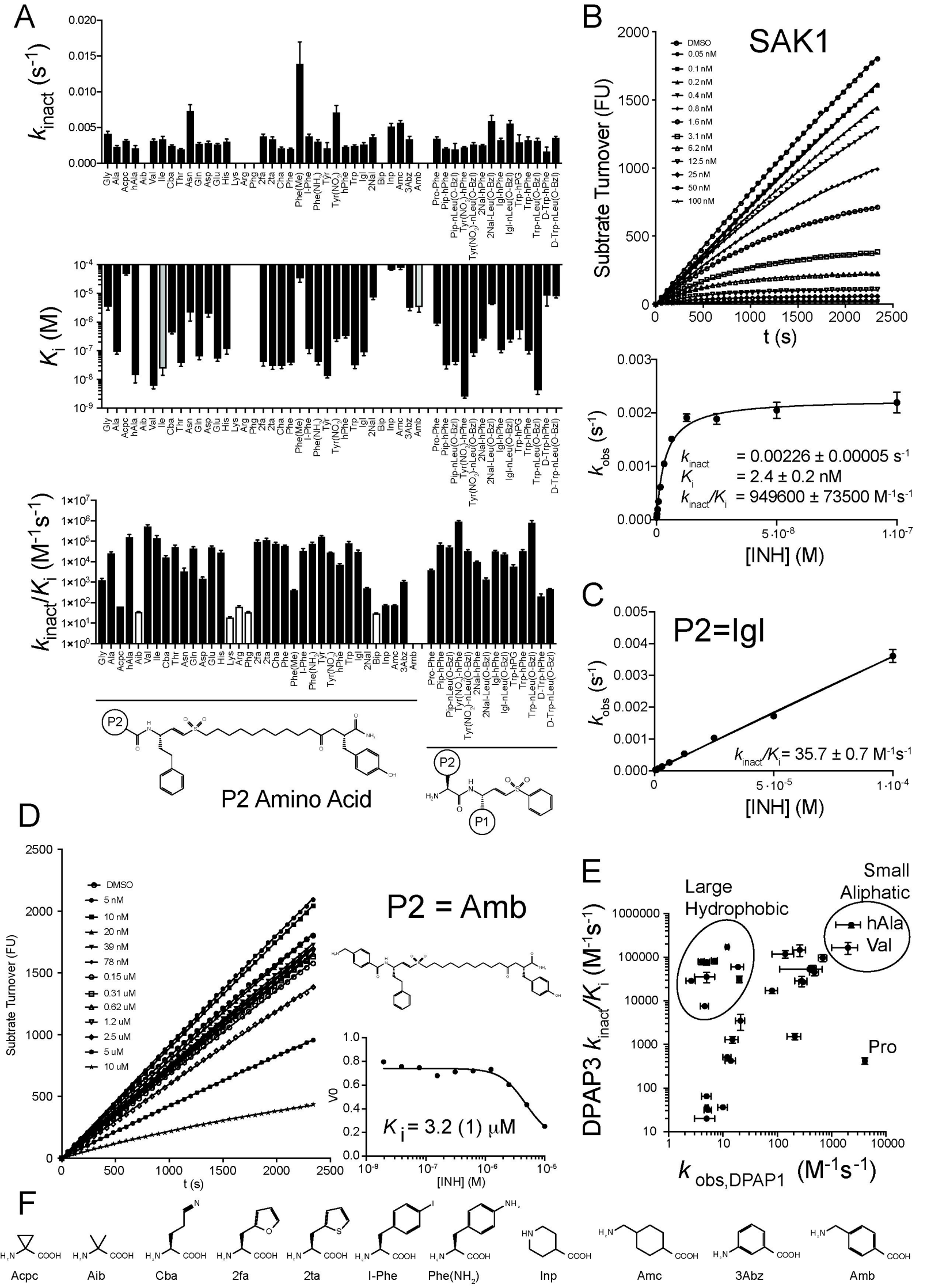
A
k_{inact} (s^{-1})
K_i (M)
k_{inact}/K_i (M^{-1}s^{-1})
Gly Ala Acpc hAla Aib Val Ile Cba Thr Asn Gln Asp Glu His Lys Arg Phg 2fa 2ta Cha Phe Phe(Me) I-Phe Phe(NH$_2$) Tyr Tyr(NO$_2$) hPhe Trp Igl 2Nal Bip Inp Amc 3Abz Amb Pro-Phe Pip-hPhe Pip-nLeu(O-Bzl) Tyr(NO$_2$)-hPhe Tyr(NO$_2$)-nLeu(O-Bzl) 2Nal-hPhe 2Nal-Leu(O-Bzl) Igl-hPhe Igl-nLeu(O-Bzl) Trp-hPG Trp-hPhe Trp-nLeu(O-Bzl) D-Trp-hPhe D-Trp-nLeu(O-Bzl)
P2
P2 Amino Acid
P1
B
SAK1
DMSO
0.05 nM
0.1 nM
0.2 nM
0.4 nM
0.8 nM
1.6 nM
3.1 nM
6.2 nM
12.5 nM
25 nM
50 nM
100 nM
Subtrate Turnover (FU)
t (s)
k_{obs} (s^{-1})
k_{inact} = 0.00226 ± 0.00005 s^{-1}
K_i = 2.4 ± 0.2 nM
k_{inact}/K_i = 949600 ± 73500 M^{-1}s^{-1}
[INH] (M)
C
P2=Igl
k_{obs} (s^{-1})
k_{inact}/K_i= 35.7 ± 0.7 M^{-1}s^{-1}
[INH] (M)
D
P2 = Amb
DMSO
5 nM
10 nM
20 nM
39 nM
78 nM
0.15 uM
0.31 uM
0.62 uM
1.2 uM
2.5 uM
5 uM
10 uM
Subtrate Turnover (FU)
t (s)
V0
K_i= 3.2 (1) μM
[INH] (M)
E
Large Hydrophobic
Small Aliphatic
hAla
Val
Pro
DPAP3 k_{inact}/K_i (M^{-1}s^{-1})
$k_{obs,DPAP1}$ (M^{-1}s^{-1})
F
Acpc
Aib
Cba
2fa
2ta
I-Phe
Phe(NH$_2$)
Inp
Amc
3Abz
Amb

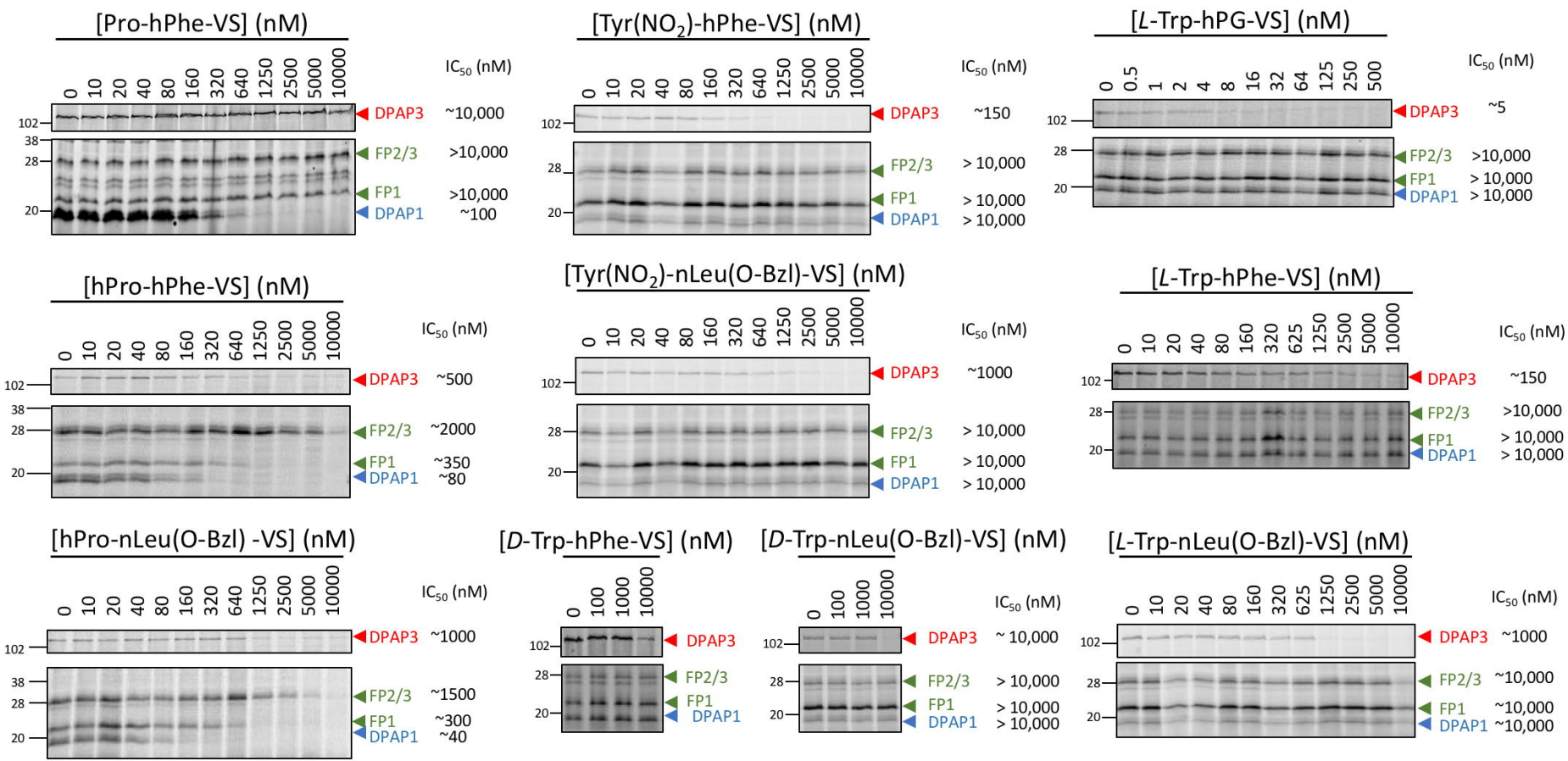
[Pro-hPhe-VS] (nM)
0 10 20 40 80 160 320 640 1250 2500 5000 10000
IC50 (nM)
102
38
28
20
DPAP3 ~10,000
FP2/3 >10,000
FP1 >10,000
DPAP1 ~100
[Tyr(NO2)-hPhe-VS] (nM)
0 10 20 40 80 160 320 640 1250 2500 5000 10000
IC50 (nM)
102
28
20
DPAP3 ~150
FP2/3 > 10,000
FP1 > 10,000
DPAP1 > 10,000
[L-Trp-hPG-VS] (nM)
0 0.5 1 2 4 8 16 32 64 125 250 500
IC50 (nM)
102
28
20
DPAP3 ~5
FP2/3 >10,000
FP1 > 10,000
DPAP1 > 10,000
[hPro-hPhe-VS] (nM)
0 10 20 40 80 160 320 640 1250 2500 5000 10000
IC50 (nM)
102
38
28
20
DPAP3 ~500
FP2/3 ~2000
FP1 ~350
DPAP1 ~80
[Tyr(NO2)-nLeu(O-Bzl)-VS] (nM)
0 10 20 40 80 160 320 640 1250 2500 5000 10000
IC50 (nM)
102
28
20
DPAP3 ~1000
FP2/3 > 10,000
FP1 > 10,000
DPAP1 > 10,000
[L-Trp-hPhe-VS] (nM)
0 10 20 40 80 160 320 625 1250 2500 5000 10000
IC50 (nM)
102
28
20
DPAP3 ~150
FP2/3 >10,000
FP1 > 10,000
DPAP1 > 10,000
[hPro-nLeu(O-Bzl) -VS] (nM)
0 10 20 40 80 160 320 640 1250 2500 5000 10000
IC50 (nM)
102
38
28
20
DPAP3 ~1000
FP2/3 ~1500
FP1 ~300
DPAP1 ~40
[D-Trp-hPhe-VS] (nM)
0 100 1000 10000
102
28
20
DPAP3
FP2/3
FP1
DPAP1
[D-Trp-nLeu(O-Bzl)-VS] (nM)
0 100 1000 10000
IC50 (nM)
102
28
20
DPAP3 ~ 10,000
FP2/3 > 10,000
FP1 > 10,000
DPAP1 > 10,000
[L-Trp-nLeu(O-Bzl)-VS] (nM)
0 10 20 40 80 160 320 625 1250 2500 5000 10000
IC50 (nM)
102
28
20
DPAP3 ~1000
FP2/3 ~10,000
FP1 ~10,000
DPAP1 ~10,000